

Search for γ -Ray Point Sources with Energy Greater Than 40 GeV along the Galactic Plane by Airborne Experiment

R. Enomoto,⁽¹⁾ J. Chiba,⁽¹⁾ K. Ogawa,⁽¹⁾ T. Sumiyoshi,⁽¹⁾ F. Takasaki,⁽¹⁾ T. Kifune,⁽²⁾
and Y. Matsubara⁽²⁾

⁽¹⁾National Laboratory for High Energy Physics (KEK), Ibaraki 305, Japan

⁽²⁾Institute for Cosmic Ray Research (ICRR), University of Tokyo, Tokyo 188, Japan

(Received 2 January 1990)

γ -ray-initiated shower cascades in the atmosphere were observed by a detector with an angular resolution of approximately 1° loaded on a cargo airplane. The γ -ray threshold was estimated to be 40 GeV. A peak search was carried out in the region of $-40^\circ < l < 80^\circ$, $-30^\circ < b < 30^\circ$ with a bin size of $2^\circ \times 2^\circ$. We observed nine γ -ray point-source candidates. Of these, eight sources were distributed along the galactic plane. The strongest source candidate (4.4σ peak) was located at $(l, b) = (39^\circ, 2^\circ)$. The integral intensities of these sources were typically several times $10^{-8} \text{ cm}^{-2} \text{ s}^{-1}$ at 40 GeV.

PACS numbers: 95.85.Qx, 98.70.Rz

In the 1970s, two γ -ray satellites, SAS II and COS-B, observed diffuse γ -ray emissions (energy range from 100 MeV to 5 GeV) from the galactic plane and discovered approximately twenty point sources, listed in the 2CG catalog.¹ Among them, only two sources (Crab pulsar and Vela pulsar) have been identified from timing correlations. Measurements with angular resolution better than 1° have been necessary in order to identify those sources with object seen via radio, optical, and x-ray observations. In the higher-energy region (from 1 TeV to 1 PeV), observations have been done by ground-based experiments with less conclusive results.² In order to fill the gap between 1 GeV and 1 TeV, we have developed a new method to measure γ rays with energy greater than 40 GeV from point sources.

A lead-glass-based electron telescope (VEGA detector), which is shown in Fig. 1, was loaded on an airplane to detect secondary electrons in a cascade shower initiated by a γ ray in the upper atmosphere. It consists of two layers of hodoscopes, a Pb converter, scintillators, and a lead-glass array. The hodoscopes are made of two XY planes which are separated vertically by 1 m. Its segmentation is 2 cm in order to obtain the angular resolution of better than 1° . The field of view is widely opened (2.03 sr geometrically and 0.935 sr for the zenith-angle distribution of $\cos^2\theta$). Between the lead glass and the lower hodoscopes, the Pb converter of 1.5 radiation lengths and scintillators (hadron scintillators) are inserted in order to reject hadron backgrounds. The lead-glass array consists of 98 modules (DF6 of $120 \times 120 \times 300 \text{ mm}^3$), covering a total area of 1.41 m^2 .³

Airplanes (Boeing B747F) are capable of flying over an altitude range from 9 to 13 km. The multiplicities of secondary electrons ($> 1 \text{ GeV}$) at 300 mbar (10 km by the zenith angle of 30°) have been calculated by EGS4 simulation as $N(e) = 0.0083 \times [E_0 / (1 \text{ GeV})]^{1.27}$, for the energy (E_0) of incident γ rays between 50 GeV and 1 TeV.⁴ The lateral spread of shower electrons ($E > 1$

GeV) is approximately 30 m. Therefore, the effective area was given by the detector area multiplied by $N(e)$. The energy threshold for incident photons was approximately 40 GeV at a 1-GeV electron-energy threshold.

The thickness of aluminum above the main deck is an average of 3 cm for the B747F. The temperature and the pressure are well controlled ($23 \pm 1^\circ \text{C}$, 0.7 atm) and ac power (110 V, 400 Hz) is available. The direction, position, and altitude of the airplane are recorded on a magnetic tape every second, with the ambiguities less than 0.5° , $0.05(1+T)^\circ$ (T in integrated flight time in hours), and 100 ft, respectively.⁵ The direction of secondary electrons was smeared from the incident photon axis by multiple scattering and by a geomagnetic field. By adding all of the contributions quadratically, the angular resolution was estimated to be 0.86° .

The hadron-rejection probability was estimated by a beam experiment to be 95%, with a loss of only 7% of the electrons. With the Pb converter, the energy resolution of the lead-glass counter is estimated to be 10% at 1 GeV. The relative gain of those counters was adjusted within 2.3% by the electron beam at the KEK accumulation ring and cosmic rays.

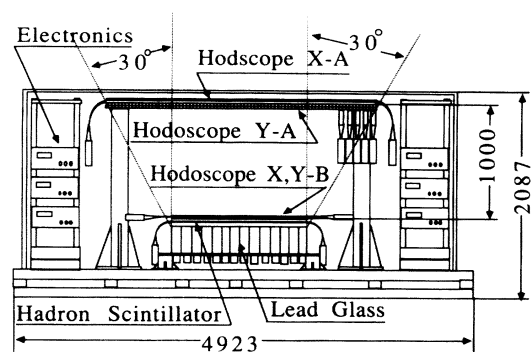


FIG. 1. Cross-sectional view of the VEGA detector.

The background due to atmospheric γ rays has been measured by the balloon-borne experiment and is formulated as $F(E) = 1.19 \times 10^{-4} [(100 \text{ GeV})/E]^{2.72} \text{ cm}^{-2} \text{ s}^{-1} \text{ GeV}^{-1} \text{ sr}^{-1}$ at 4 mbar.⁶ We assumed that the probability of the γ -ray ($\pi^0 \rightarrow \gamma\gamma$) production is proportional to $e^{-t/\Lambda}$, where t is an atmospheric depth and Λ is an interaction length (~ 100 mbar). The trigger rate at 260 mbar (10 km) was estimated to be 48 Hz when the trigger threshold was set to 800 MeV and the background counts in a 10^{-3} -sr window was 142 counts/h at the 1-GeV software threshold.⁷ For the γ -ray point sources with the integral intensity of $J_s(E) \geq 5 \times 10^{-7} E^{-1} \text{ cm}^{-2} \text{ s}$, such as the Vela pulsar and Geminga, the expected yield is ≥ 11 counts/h in the 10^{-3} -sr window.¹ We can therefore obtain a $\geq 90\%$ -C.L. upper limit by 3-h observation and a $\geq 5\sigma$ signal by 30 h.

On 7 June 1989 (JST), we carried out the first flight between Narita (Japan) and Sydney (Australia), via Guam. The flight numbers were JAL 661 and 662 (Japan Air Lines Co. Ltd.) which departed from Narita at 6 a.m., 7 June (JST). The main data presented in this paper were obtained on the flight from Sydney to Guam, viewing the galactic center region. The trigger mode was the coincidence of the hodoscopes and the lead glass with energy deposit (> 800 MeV). The trigger rate was 60 Hz (=50 Hz of electrons + 10 Hz of protons), consistent with the estimations so far known.⁸

In the off-line data reduction, we selected the lower-multiplicity events in order to reject the conversion events at the airplane ceiling. The cutoff number of total track candidates ($N_h = N_{X-A} N_{Y-A} N_{X-B} N_{Y-B}$) in the hodoscopes was set to $N_h < 20$. By a Monte Carlo simulation, low-energy electrons (photons) are emitted from the airplane ceiling, the Pb convertor, and the lead-glass detector and they are expected to hit the hodoscopes. The mean value of N_h is estimated to be 11.7 and the cut at 20 contains 85% of the events. The electromagnetic clusters were reconstructed independently by the lead-glass array. The neighboring hits were combined with the cluster and the hit positions of the cluster were defined by the center of gravity of the pulse heights. The position resolution was typically 40 mm. The energy threshold for the lead-glass cluster was set to 800 MeV, corresponding to a 1-GeV threshold at the airplane injection. The cluster in the hadron scintillators was reconstructed in the same way. The X position was obtained by calculating the center of gravity over the segments and the Y position was obtained by the pulse-height ratio of two photomultipliers in both ends. The resolutions were 25 and 105 mm, respectively. Electrons, in most cases, make cascades in the Pb convertor and deposit large energies in the hadron hodoscope, while protons do not. Thus, the proton component was rejected by the pulse height of the cluster. The threshold for electron candidates was set to $dE > 2.3$ times the value of the minimum ionizing track. The proton sample thus reject-

ed was used for a background study. The final track fitting was performed by a χ^2 minimization. The χ^2 cut was set to 25, where the number of degrees of freedom was four. The best χ^2 solution associated with a lead-glass cluster was selected as an electron candidate. The reconstruction efficiency was calculated to be 47%. After selection, 96.5% of the events had a single track.

In order to check the detector resolution and the method itself, we analyzed double-track events by relaxing the selection criteria, namely, the total number of track candidates from 20 to 400. Tracks were considered to come from the same shower, so that both must have the same direction within the resolution. Two tracks were parallel in $\frac{1}{3}$ of the double-track events and the angular resolution obtained from the mean angular difference for those events was $0.98^\circ \pm 0.09^\circ$ which was slightly larger than our previous estimation. The final angular resolution including all of the effects was considered to be $1.2^\circ \pm 0.1^\circ$. It was concluded that the telescope detected the air-shower particles and the measured angle gave the correct directions of the incident γ ray.

The sensitive area in the galactic coordinate (l denotes galactic longitude, b denotes galactic latitude) was the region of $-40^\circ < l < 80^\circ$ and $-30^\circ < b < 30^\circ$, where an exposure time was greater than 1.3 h. The incident directions of electrons were calculated in this area and the peaks of events were searched by a $2^\circ \times 2^\circ$ binning (1800 bins in total). The control background was made by averaging and smoothing the neighboring b slices. In the $-6^\circ < b < 6^\circ$ region, the width of the distribution of $(N - N_{bg})/\sqrt{N}$ for each bin was 30% wider on the positive side than the normal distribution while that on the negative side is consistent with it, suggesting that signals existed in the data set along the galactic plane. The number of the excessed bins ($> 3\sigma$) in the electron sample was six and that in the proton sample was zero. On the other hand, the distribution for the other b region was consistent with the normal distribution. The distribution for the proton sample in the entire b region was also consistent with the normal distribution.

The excesses beyond the background were searched for by picking up the peaks of statistical significance greater than 1.5σ , 2.5σ , and 3.5σ ; the b projections of those peak candidates are plotted in Figs. 2(a), 2(b), and 2(c), respectively. Histograms are experimental data and curves are obtained by a Monte Carlo simulation. The peak distributions agreed well with the Monte Carlo simulation for the lower σ cuts and deviated significantly for higher σ cuts, especially in the $-6^\circ < b < 6^\circ$ region, i.e., in the galactic plane. In Fig. 2(c), we observed nine peaks, eight of which were in the above region, while the Monte Carlo simulation predicted 0.9 peak. A Poisson fluctuation gave the probability of an occurrence to be 4.9×10^{-6} . There is a possibility that the "sources" are actually fluctuations of a broad excess from the direction of the galactic plane. Outside the galactic plane, data

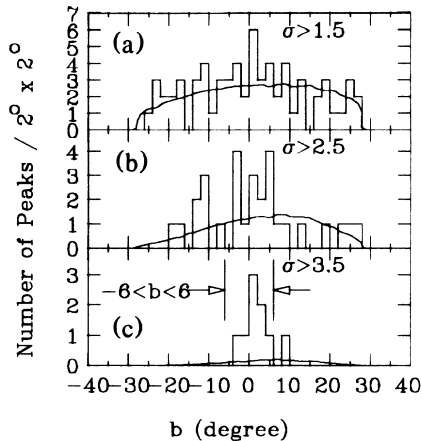


FIG. 2. Number of peaks obtained by the cluster-finding algorithm described in the text. The figures are the b distributions of those peaks: (a), (b), and (c) were obtained by a different statistical significance cut, i.e., 1.5σ , 2.5σ , and 3.5σ , respectively. Histograms were experimental data and curves were Monte Carlo calculations.

and the Monte Carlo simulation agreed well. We carried out the same analysis for the proton sample, but observed no peak in the entire b region by a 3.5σ cut. In addition, we applied the same procedures to the data obtained in the flight from Guam to Sydney when the galactic anticenter region was in the field of view. However, there was a minor problem in recording the directional data for the airplane in this region and only half of the data were used in the analysis. We observed two peaks and one peak by a 3.5σ cut for electron and proton samples, respectively, consistent with statistical fluctuation.

The l distributions of the electron sample inside and outside the galactic plane are shown in Fig. 3 for eight different b slices. The histograms are experimental data and the dashed curves are the control background obtained by the method described above. The peak identified by the above criteria of the 3.5σ cut were tagged with capital letters.

In Table I, the characteristics of the observed peaks, such as the numbers of entries and the positions in the galactic coordinate, are summarized. These numbers were obtained by refitting the l distribution in Fig. 3 with a fifth-order polynomial plus multiple Gaussians with the point-spread function ($\sim 1.2^\circ$). The systematic error in the position determination was considered to be less than 1° , with the largest error in the detector alignment with the airplane axis. Two peaks have relatively stronger statistical significances, i.e., source A and source B. The latter is within the error box of the hard- γ -ray point source, 2CG359-00, but 2σ away from the galactic center.¹ The other sources are far from the COS-B sources by more than 2° . Source A has a broader width in the b direction, as seen in Fig. 3. For source B, the observed flux was of a similar amount when the data set

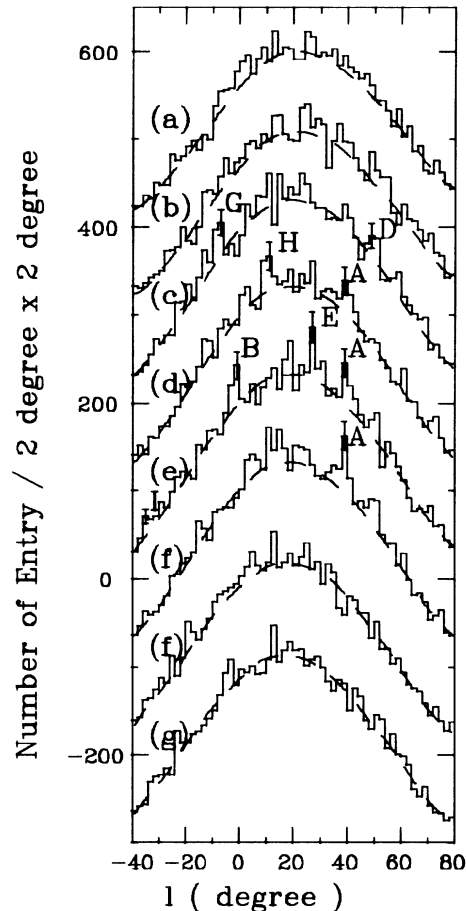


FIG. 3. Distributions of l of electrons, in the 2° slices of b with vertical offset values in the parentheses: (a) $-14^\circ < b < -12^\circ$ (400), (b) $-12^\circ < b < -10^\circ$ (300), (c) $-4^\circ < b < -2^\circ$ (200), (d) $-2^\circ < b < 0^\circ$ (100), (e) $0^\circ < b < 2^\circ$ (0), (f) $2^\circ < b < 4^\circ$ (-100), (g) $10^\circ < b < 12^\circ$ (-200), and (h) $12^\circ < b < 14^\circ$ (-300). The histograms are the incident directions (l) of electrons. The dashed curves are the control backgrounds which are described in the text. The peaks found by the algorithm described in the text are tagged with the symbols A, B, D, E, G, H, and I in Table I. The error bars are statistical ones.

was divided into two runs of the first 2 h and the rest. The differential energy spectrum was obtained to be $E^{-\gamma}$ ($\gamma = 1.8 \pm 0.8$) for source B.

The primary integral intensities of those sources at 40 GeV were estimated by using the shower theory and EGS4 simulation. The incident integral energy spectrum was assumed to be $E^{-\gamma}$. The integral intensities at 40 GeV were obtained to be $(1.13 \pm 0.26) \times 10^{-7}$ ($\gamma = 1.0$), $(2.19 \pm 0.50) \times 10^{-7}$ ($\gamma = 1.4$), and $(1.31 \pm 0.30) \times 10^{-7}$ $\text{cm}^{-2}\text{s}^{-1}$ ($\gamma = 2.0$) for source A and $(0.64 \pm 0.17) \times 10^{-7}$ ($\gamma = 1.0$), $(1.47 \pm 0.39) \times 10^{-7}$ ($\gamma = 1.4$), and $(1.04 \pm 0.27) \times 10^{-7}$ $\text{cm}^{-2}\text{s}^{-1}$ ($\gamma = 2.0$) for source B. The intensity is consistent with the extrapolations of those of Vela pulsar and Geminga observed by the

TABLE I. The characteristics of the peak candidates. The error radius of those point sources is estimated to be $\pm 1.0^\circ$.

Peak	Number of events	Position l, b (deg)	Exposure time (h)
A	136 ± 31	39.4, +2.1	2.92
B	84 ± 22	358.2, +1.0	3.16
C	105 ± 30	32.8, +6.1	3.20
D	96 ± 28	50.2, +2.1	2.37
E	98 ± 30	27.1, +0.5	3.33
F	69 ± 23	4.0, +9.0	3.18
G	61 ± 21	352.4, -3.0	2.96
H	64 ± 22	10.1, -1.0	3.46
I	28 ± 11	325.4, +1.0	1.38

COS-B satellite, but significantly higher than those of the other COS-B sources and that of the Crab nebula at 1 TeV.⁹ If the energy spectra were hard ($\gamma \sim 1.0$), these sources should be easily detected by air Cherenkov experiments. For source B, the luminosity in the energy region from 40 GeV to 1 TeV was calculated for the $\gamma = 1$ case to be $(7.4 \pm 2.0 \pm 1.9) \times 10^{36}$ ergs/s by assuming that the distance of the source is 8 kpc (i.e., the galactic center).

A new method for measuring high-energy γ rays from astronomical objects has been developed and been proved to be useful. The energy threshold was 40 GeV and the angle resolution of γ rays was approximately 1° . We observed nine point-source candidates and eight sources were along the galactic plane. The strongest source candidate was located at $(l, b) = (39^\circ, 2^\circ)$ and the flux was

as large as $10^{-7} \text{ cm}^{-2} \text{ s}^{-1}$ above 40 GeV. Further confirmation is necessary.

We appreciate support from Professor J. Nishimura (International School for Advanced Studies), Professor H. Sugawara, Professor K. Kikuchi, Professor K. Takahashi, Professor S. Iwata, Y. Ukita (KEK), Professor T. Kamae, Dr. T. Takahashi (University of Tokyo), Professor J. Arafune (ICRR), Dr. Y. Takahashi (NASA, Alabama), Hamamatsu Photonics K. K., and Japan Air Lines Co. Ltd.

¹G. F. Bignami and W. Hermsen, *Annu. Rev. Astron. Astrophys.* **21**, 67 (1983); H. A. Mayer-Hasselwander and G. Simpson, in *Proceedings of the Twenty-First International Cosmic Ray Conference, Adelaide, Australia, 1989*, edited by R. J. Protheroe (Graphic Services, Northfield, 1990), Vol. 1, p. 261.

²R. C. Lamb, in *Proceedings of the Thirteenth Texas Symposium on Relativistic Astrophysics, Chicago, 1986*, edited by M. P. Ulmer (World Scientific, Singapore, 1987), p. 589.

³K. Ogawa *et al.*, *Nucl. Instrum. Methods Phys. Res., Sect. A* **243**, 58 (1986).

⁴W. R. Nelson *et al.*, SLAC Report No. 265, 1985 (unpublished).

⁵M. Iizuka, Japan Air Lines Co. Ltd. (private communication).

⁶J. Nishimura *et al.*, *Astrophys. J.* **238**, 394 (1980).

⁷R. Enomoto *et al.*, KEK report No. 89-55, 1989 (to be published).

⁸S. Hayakawa, *Cosmic Ray Physics* (Wiley, New York, 1969).

⁹T. C. Weekes *et al.*, *Astrophys. J.* **342**, 379 (1989).